



EFFECTS OF INJECTION TIMING OF DIESEL FUEL ON PERFORMANCE AND EMISSION OF DUAL FUEL DIESEL ENGINE POWERED BY DIESEL/E85 FUELS

Wojciech TUTAK^{1*}, Arkadiusz JAMROZIK², Ákos BEREZKY³, Kristof LUKACS⁴

^{1,2}*Faculty of Mechanical Engineering and Computer Science,
Czestochowa University of Technology, Poland*

^{3,4}*Dept of Energy Engineering, Budapest University of Technology and Economics, Hungary*

Received 8 July 2016; revised 5 October 2016, 14 November 2016; accepted 3 December 2016

Abstract. The paper presents the results of the investigation of Dual Fuel (DF) diesel engines powered by high bioethanol contain fuel – E85. The object of the investigation is a three-cylinder Compression Ignition (CI) Internal Combustion Engine (ICE) powered by diesel oil and bioethanol fuel E85 injected into the intake port as a DF engine. With the increase in the share of E85 fuel the highest intensification of the combustion process takes place in the main stage of the combustion and the ignition delay increases as well. The researchers are conducted using Computational Fluid Dynamics (CFD) method; the results of the investigation are successfully verified based on the indicator diagrams, heat performance rate and emissions. Based on CFD results the cross sections investigation of the combustion chamber it can be seen that in case of the DF engine, the flame front propagates with a higher speed. The initial phase of the combustion starts in a different location of the combustion chamber than in the classic CI engine. Replacement of diesel fuel by E85 in 20% resulted in the shortening of the combustion duration more than 2-times. With the increase of energetic share in E85 the soot emission is decreased at all ranges of the analysed operations of the engine. The opposite relationship was observed in case of NO emission. With the increase of E85 in the fuel, the emission of NO increased.

Keywords: dual fuel engine, diesel engine, exhaust emission, modelling, combustion.

Notations

aTDC – after top dead center [deg];
bTDC – before top dead center [deg];
BDC – bottom dead center [deg];
CA – crank angle [deg];
CFD – computational fluid dynamics;
CI – compression ignition;
CNG – compressed natural gas;
CO – carbon monoxides;
CO₂ – carbon dioxides;
DF – dual fuel;
ECFM – extended coherent flame model;
EGR – exhaust gas recirculation;
EVC – exhaust valve closing [deg];
EVO – exhaust valve opening [deg];
HC – hydrocarbons;
HCCI – homogeneous charge compression ignition;
HRR – heat release rate [J/deg];
ICE – internal combustion engine;

IMEP – indicated mean effective pressure [MPa];
IT – injection timing [deg];
ITE – indicated thermal efficiency [%];
IVO – intake valve opening [deg];
IVC – intake valve closing [deg];
NO – nitric oxides;
NO_x – nitrogen oxides;
PM – particulate matter;
PRR – pressure rise rate;
RME – rapeseed methyl ester;
T – temperature [K];
TDC – top dead center.

Introduction

The CI (diesel) engines are widely used due to their relatively high efficiency at full and partial load conditions and long lifetime. The Directive 2009/28/EC (EC 2009)

*Corresponding author. E-mail: tutak@imc.pcz.czest.pl

approved a target of a 20% share of renewable biofuels in overall transport petrol and diesel consumption by 2020 to be introduced in a cost-effective way. The main reasons of using biofuels are lower greenhouse gas emissions and diversification, which cause increase energy independence and reduce consumer reliance on imported fossil fuels and depleting oil reserves (Labeckas *et al.* 2014). Recently, increasing attention has been paid to the use of non-petroleum-based fuels made from biological sources, including alcohols (predominantly ethanol), as important liquid biofuels (Sarathy *et al.* 2014). There are many types of renewable fuels for diesel engines. Possible fuels are the different biodiesels from edible and from non-edible raw materials with different esterification technologies. Among alternative fuels, alcohols are recently considered as most promising. Alcohols due to their nature are included in the oxygenated fuels (Rakopoulos *et al.* 2008a, 2008b). Alcohol fuels are applicable to diesel combustion engines and these are to contribute significantly to petroleum-based fuels as substitutes. One of alcohol fuels is ethanol C_2H_5OH . In some countries, it is available in the form of E85. It is a mixture of ethanol and gasoline in a volume ratio of 85/15. In practice there are a few methods involving alcohol diesel combustion. CI engine with ethanol fuel engine can operate in different methods (Abu-Qudais *et al.* 2000; Zöldy, Török 2015; Şahin, Durgun 2013; Padala *et al.* 2013; Vallinayagam *et al.* 2014; Zhang *et al.* 2009, 2010): alcohol-diesel blend – mixing the fuels just prior to injection, alcohol diesel emulsion – emulsifier to prevent the separation of fuels, alcohol fumigation – alcohol is fumigated to the intake air system, dual injection – separated injection systems. The fumigation method is required in addition to an injector along with a separate fuel tank, lines and control unit. Alcohol can be introduced by a carburettor, a vapouriser or an injector. The most popular method is the utilization of an injection system of a spark ignition engine because of the low price and easy access. In this technology, the main fuel is delivered into the intake port of the engine. During the intake stroke, an almost homogeneous mixture is created and at the end of the compression stroke, this mixture is ignited by direct injection of the diesel fuel into the combustion chamber. The start of the combustion is controlled by timing of the injection of diesel fuel. One advantage of this method is the omission of the separation of phases. Another advantage of this system is the possibility of the engine work as only a diesel engine. The engine can be switched from DF to diesel fuel operation by disconnecting and connecting the intake manifold injector system. This is important by low temperature conditions of the engine. The engine can be started as a diesel engine and then, after warming up, it can start to work as a DF engine. The first technical solution is related to DF technology for engines fuelled with CNG (Luft 2010; Wei, Geng 2016). Alternative fuel burning in a diesel engine has a great potential to achieve highly efficient combustion with low exhaust emissions such as systems with both homogenous charge CI and stratified charge CI (Jamrozik, Tutak 2011, 2014). The available

methods of PM and NO_x reduction include engine modifications as well as after-treatment of exhaust gases or EGR systems (Jamrozik, Tutak 2010; Tutak, Jamrozik 2011). Authors of the recent work studied and compared a variety of fuels and bio-fuels and their effects on the combustion process and emission (Wei, Geng 2016; Tutak *et al.* 2014, 2015; Tutak, Jamrozik 2014; Jamrozik *et al.* 2013; Irimescu *et al.* 2015; Merola *et al.* 2014; Valentino *et al.* 2014; Jamrozik 2009). Ethanol is usually associated with a spark-ignition engine because of its high octane number. For several years, ethanol has been considered as a fuel for diesel engines (Zöldy 2011; Şahin *et al.* 2015; Morsy 2015; Sayin, Canakci 2009; Sarjoovaara *et al.* 2013). The paper of Can *et al.* (2004) investigated the effect of ethanol addition to diesel fuel on the performance and emissions of turbo-charged diesel engines. They stated that ethanol addition reduced CO and soot emissions although it caused an increase in NO_x emission and power reductions. Abu-Qudais *et al.* (2000) investigated and compared the effects of ethanol fumigation and ethanol-diesel fuel blends on the performance and emissions of a single cylinder diesel engine. The results showed that both the fumigation and blend methods have the same behaviour in affecting performance and emissions, but the improvement in using the fumigation method was better than blends. They stated that the optimum percentage for ethanol fumigation was 20% (Abu-Qudais *et al.* 2000). In case of emission, they reached an increase in CO (55%) and HC (36%) but a reduction of soot (51%) concentration. The optimum percentage for ethanol-diesel fuel blends was 15%. This produces an increase of 43.3% in CO (43%) and HC (34%) and a reduction of soot (32%) concentration (Abu-Qudais *et al.* 2000). Padala *et al.* (2013) in their work presented the results of the potential of ethanol fuelling in a diesel engine to achieve higher efficiency. They found that increased ethanol energy fraction increases the engine efficiency until the operation is limited by misfiring associated with over-retarded combustion phasing. By energy fraction, up to 60% of diesel is replaced by ethanol, which achieves an efficiency gain of 10% compared to diesel-only operation. They stated also that the decreased burn duration is the primary cause for the efficiency gain, i.e. the fast burning of ethanol improves the combustion. As a fuel for diesel engine *n*-butanol is considered as well. Siwale *et al.* (2013) in their work presented the results of burning of 5%, 10%, and 20% shared volume of *n*-butanol with DF in a high load, light duty, turbo-charged diesel engine. They stated that NO_x emission increased by 10.3, 32.3 and 54.4% above DF at 75% load at speed 1500 rpm for B5, 10 and 20 respectively. Increasing the fraction of alcohol content in the blend reduced CO emission. Unburned HC are reduced significantly using *n*-butanol/DF blends. They also stated that it was a more appreciable premixed combustion phase with increased *n*-butanol/DF shared volume. They explain that there occurs an increased effectiveness of air-fuel mixing during the ignition delay period. There are also works on the use of gasoline as a fuel to power diesel engines in DF system

(Ma *et al.* 2013). The experimental results showed that this combustion mode had the capability of achieving high efficiency with a nearly zero NO_x and soot emissions by using an early IT of single strategy with high fuel ratio. They stated that in single injection strategy, the combustion characteristic of single injection strategy with high gasoline ratio was similar to HCCI, so the ultra-low NO_x and soot emissions were achieved simultaneously. The emissions of NO_x and soot were very low but they noticed significant increase in HC and CO emissions. In the paper (Rakopoulos *et al.* 2008a, 2008b) the authors presented a comprehensive, two dimensional, multi-zone model which has been developed for direct injection diesel engines and applied for the cases of using two different fuels: neat diesel fuel and a blend of ethanol–diesel fuel with 15% (V/V%) ethanol. The model follows each zone, with its own time history, as the spray penetrates into the swirling air environment of the combustion chamber. The modelling results showed that the high fuel to air equivalence ratio areas within the fuel spray are limited when using ethanol–diesel fuel blends instead of diesel fuel, a fact attributed to the oxygen bound in the fuel that is progressively released as the oxygenated fuel is evaporated. Sarjovaara, Larmi (2015) and Sarjovaara *et al.* (2015) investigated the ethanol/gasoline blend E85 as the primary fuel in a dual-fuel co-combustion process. The E85 blend was injected into the intake manifold and the mixture was ignited by a diesel fuel injection bTDC. They investigated the effect of charge air temperature on E85 ethanol/gasoline blend dual-fuel combustion. The combustion process was studied with minimum modifications to the engine. They stated that charge air temperature influenced the ignition delay, the cylinder PRR and the maximum cylinder pressure by altering the E85 combustion phasing, while the changes on the diesel fuel combustion were minor. Lower charge air temperatures allowed higher E85 injection rates without the risk of a too high peak pressure rise, especially at high load conditions. The increase of the E85 rate allowed by lower charge air temperature, decreased NO_x emission, but simultaneously increased CO and unburned total HC emissions and decreased combustion efficiency. Splitter *et al.* (2014) presented the results of the modelling of a DF diesel engine powered with E85 and diesel fuel. The results demonstrated that for fixed cycle thermodynamics, sources of engine inefficiency depend on the premixed and global equivalence ratios. They stated that in order to reduce the peak PRR, leaner conditions were required, and the peak gross thermal efficiency increased. However, bioethanol fuel is not ignitable via compression in diesel engines, as it requires an ignition source. Raslavičius and Bazaras (2009, 2010) investigated the influence of blend of organic origin including RME and ethanol (E) with fossil diesel as a fuel for the unmodified high-speed diesel engine. They stated that engine-operating parameters were improved in the presence of ethanol additives in D–RME blend with a reduction in pollutant emissions in exhaust gases and fuel consumption. Jamrozik *et al.* (2017) investigated the effect of diesel/biodiesel/

ethanol blend on combustion, performance and emissions characteristics on a direct injection diesel engine. They stated that the increase in ethanol fuel in blend causes the increase in ignition delay (38.5% for full load) but burn duration decreased (49% for full load). Lebedevas *et al.* (2013) presented results of investigation of using two-component RME–E (rapeseed methyl ester – ethanol) and three-component D–RME–E biodiesels in high-speed diesel engines. They stated that heat release was transferred from two-phase to one-phase heat release and noticed an increase in the fuel's economy of the engine for every 10% increase of ethanol in the fuel. Cyclic stability of the diesel engine, operating on biodiesels containing ethanol fraction up to 30%, did not exceed those that are common for diesel engines operating on mineral diesel.

Therefore, the auto-ignition of the diesel spray can act as a pilot to ignite the premixed mixture of E85/air. In this paper, the authors attempted to model the CFD thermal cycle DF engine fuelled with diesel and E85 bioethanol fuel. For selected energetic shares of E85 the thermodynamic cycle parameters and the toxicity of exhaust gases, soot and NO will be analysed. There are many publications on ethanol utilization in CI ICE (DF or blend), but E85 can be an alternative fuel, because this high bio content fuel is available on the market. To buy E100 is not possible, this is not available on the market, only hydrous ethanol is used in Brazil. On the basis of a review of the literature (Sarjovaara *et al.* 2015; Sarjovaara, Larmi 2015; Tutak, Jamrozik 2014; Tutak *et al.* 2015) the E85 fuel is increasingly used to power CI engines. In the present study authors used the engines with these same settings as for diesel fuel powering, without any optimization. The reason for this was to determine the influence of fuel change on the combustion process. The next important step is the optimization of the engine cycle in terms of the angle of the start of combustion. In this study AVL FIRE CFD code was used to code AVL FIRE to optimization process of DF diesel engine powered by E85 fuel.

1. Object of the investigation

The object of our investigation is the 3-cylinder direct injection diesel engine, which is adapted to operate as a DF engine. Additional fuel is delivered to the intake manifold separately to each cylinder. The cylinder of the engine is filled with near homogeneous mixture, which is ignited by pilot diesel fuel injected at the end of the compression stroke. In Table 1 the main parameters of the engine are presented and the main initial conditions for the engine model. The engine is operated with a constant speed equal to 1500 rpm with full load of 24 kW. The compression ratio was equal to 17:1. The details of the measurement and the test system are described in previous works (Tutak *et al.* 2015; Tutak, Jamrozik 2014). The measurement system consists of: diesel fuel consumption – AVL 7031 gravimetric meter, exhaust emissions (NO_x , CO, HC) – Horiba Motor Exhaust Gas Analyser MEXA 8120F, exhaust emissions (CO_2 , O_2) – Sick Maihak S710 Gas Analyser, smoke

meter AVL 415, in-cylinder pressure sensor – Kistler 6001, charge amplifiers – Kistler 5001, pilot IT – piezoelectric sensor attached to the high pressure fuel pipe – Kistler 6001 with adapter – Kistler 6501, resolution for the data acquisition system – 0.35 CA deg.

In Figure 1 the system of the DF engine is presented equipped with two injector systems. The alcohol fuel IT and duration were controlled by an electronic injection controller equipped with a fuel pressure sensor. The amount of fuel supplied was controlled by injector opening time. The angle of start of diesel fuel injection for DF engine, assumed the optimum angle for engine operating on pure diesel fuel without the addition of biocomponents was 8.5 deg bTDC.

To increase E85 energy percentage, the diesel fuel dose per engine cycle was decreased by reducing the injection duration of diesel fuel, while E85 mass was increased by extending the injection duration.

Fuel properties are presented in Table 2. Some mean properties of diesel and bioethanol fuel E85 are compared therein. E85 has a lower heating value compared to diesel fuel. Another significant difference is a 3 times larger heat of vaporization of E85 compared to diesel fuel. Ethanol C_2H_5OH as a main component of E85 contains a fraction of oxygen, which results in lower stoichiometric air fuel ratio. To the power engine with such fuel, oxygen is also supplied indirectly. The fuel consumption rate with E85 is higher compared to diesel fuel because of the lower

Table 2. Properties of diesel fuel and E85 (Tutak et al. 2015; Tutak, Jamrozik 2014; Sarjovaara et al. 2015; Sarjovaara, Larmi 2015)

Properties	Diesel	E85
Molecular formula	$C_{14}H_{30}$	$C_nH_{2.88n}O$
Molecular weight	198.4	56.29
Cetane number	51	~11 (pure ethanol), 20–25 (gasoline)
Lower heating value [MJ/kg]	41.66	29.6
Density at 20 °C [kg/m ³]	856	785
Viscosity at 20 °C [mPa s]	2.8	1.2
Heat of evaporation [kJ/kg]	260	780
Stoichiometric air fuel ratio $(A/F)_{st}$	14.7	9.92
Autoignition temperature [°C]	230	420 (pure ethanol), 300 (pure gasoline)
Flame speed [m/s]	0.86	~3
Flame temperature [°C]	2054	2120 (ethanol)
Carbon content [wt %]	87	52.2 (ethanol), 85.5 (gasoline)

calorific value of alcohol. Actual air–fuel ratio decreases with increasing the E85 fraction. However, a stoichiometric air–fuel ratio of E85 is 9.92, significantly lower than diesel's 14.7. The decrease in both the stoichiometric air–fuel ratio and the actual air–fuel ratio with increasing E85 energy fraction resulted in small variations in the overall excess air ratio (Tutak et al. 2015; Tutak, Jamrozik 2014). It is a DF engine and E85 fuel is supplied to the engine with the air during the intake stroke. E85 with air create a lean mixture. As shown in Table 2, the E85 autoignition temperature is 420 °C. During the compression stroke, temperature is too low to ignite the mixture. If there have to ignite the mixture we would have to do with the HCCI engine. In our case, due to the low temperature of autoignition of diesel fuel, the injected dose of diesel fuel ignites the mixture E85/air. This gives makes the ability to control the ignition timing.

2. Background of modelling of the DF technology

Within the study, the authors examined the co-combustion of diesel and bioethanol E85 fuel used as a DF technology. The object of the investigation as a DF IC engine is realised based on a diesel engine equipped with a port fuel injection system. The analysis is based on the CFD simulation. In Figure 2 the scheme of DF combustion in the combustion chamber of a diesel engine is presented. In case of a conventional diesel engine the fuel is injected into the combustion chamber where it is surrounded by air of high thermodynamic parameters. Fuel sprays or rather droplets of diesel fuel started immediately to vapour after entering the combustion chamber.

Study of the combustion of fuel droplets in air indicated that ignition starts in the layer of vapour surround-

Table 1. Main specifications of the engine model

Power	24 kW
No of cylinders	3
Bore	104 mm
Stroke	115 mm
Engine speed	1500 rpm
Compression ratio	17:1
Displacement of cylinder	0.97 dm ³
IVO	20 deg bTDC
IVC	40 deg aBDC
EVO	40 deg bBDC
EVC	5 deg aTDC
No of nozzle holes	3

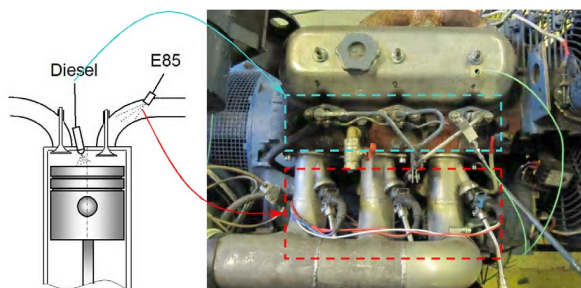


Figure 1. Fuel supply system of the DF engine and the view of the experimental setup with injection system

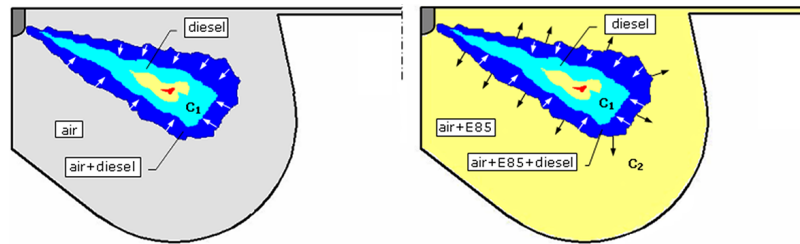


Figure 2. The scheme of diesel (a) and DF (b) combustion: C_1 – flame expansion in the diesel oil jet, C_2 – flame expansion in the E85-air mixture

ing the drop and that the combustion rate of drops was limited by their evaporation rate (Figure 2a). Burning rate decreases as the fraction of oxygen in the surrounding air decreases. In case of a DF engine droplets are surrounded by a mixture of air-fuel of higher thermodynamic parameters as previously (Figure 2b).

In a DF engine the droplets evaporation mechanism is the same as in the case of a diesel engine, but because of the relatively high value of heat of evaporation of alcohol fuel, this process can be less intense (López *et al.* 2013). Additionally the combustion process starts in the presence of air and two fuels of different parameters. The flame expansion takes place in two directions, in a diesel engine rather towards the injected cloud of diesel fuel droplets and in the other case into the combustion chamber filled with air-fuel mixture. Therefore, it is expected that in case of a DF engine the combustion process will occur faster than in case of a diesel engine. However, with an increase of second fuel participation, due to the high value of the heat of vaporization it can be noticed misfires or a depletion of the combustion process.

3. Model assumptions

The model studies are based on the ECFM combustion model (AVL LIST GmbH 2013). The used code is developed based on the finite volume approach with the pressure based segregated solution algorithm and the SIMPLE algorithm is used for pressure-velocity coupling in the solution procedure. For modeling the diesel combustion process, we used the ECFM-3Z model and in case of DF mode we used CFM with a diesel ignited gas engine model (Colin, Benkenida 2004). In Table 3 the used sub-models are presented.

The turbulence of charge and turbulent wall heat transfer is modelled using the $k-\zeta-f$ turbulence model. The hybrid wall treatment model is used to ensure a

gradual change between viscous sub-layer formulations and the wall functions. The spray is modelled with the use of WAVE breakup model (Kim *et al.* 2005), which determined the size of droplets in the spray on the basis of the wave length of the speed of the droplets. The evaporation process is modelled with the use of the Dukowicz model. The ECFM is developed specially for modelling the combustion process in a CI engine. The CFM has been successfully used for modelling the process of combustion in spark ignition engines. This model belongs to a group of advanced models of the combustion process in a CI engine. Together with turbulence process sub-models (e.g. the $k-\zeta-f$), exhaust gas component formation, knock combustion and other sub-models, which constitute as a useful tool for the modelling and analysis of the thermal cycle of the CI ICE. To adapt the model for the modelling of the combustion process in the CI engine, a sub-model has been added, which describes the process of mixing fuel to be injected to the combustion chamber. The turbulent combustion process is defined by the time scale of chemical reactions, the time scale of turbulent processes, and turbulence intensity. The flame front is formed by the turbulent effect of load vortices and the interaction between the burned zone and the unburned part of the load. This model is based on the concept of laminar flame propagation with flame velocity and flame front thickness as the average flame front values. It is also assumed that the reactions occur in a relatively thin layer separating unburned gases from the completely burned gases. The model relies on the flame front transfer equation, as well as on the mixing model describing the combustion of an inhomogeneous mix and the diffusion combustion model. The ECFM with a diesel ignited gas engine model combines homogeneous premixed gas combustion with diesel ignition. It is possible to use the Eddy Breakup combustion model or the ECFM combustion model for the main burning phase. In case of a DF engine the auto-ignition is calculated in regions which are richer than the homogeneous mixture (AVL LIST GmbH 2013). The program calculates the mean fuel mass fraction in the whole domain and uses this value as a limit for cells with auto-ignition. The injection function profile was taken from an experiment which was recorded as a pressure injection history (Figure 3). This made measurements by a piezo-electronic transducer on the high pressure line of injector No 1 (Figure 1).

Boundary and initial conditions for the cylinder walls, valves and intake and exhaust manifolds channels

Table 3. Sub-models for calculations (AVL LIST GmbH 2013)

ECFM-3Z, ECFM combustion model
$k-\zeta-f$ turbulence model
WAVE breakup model
Dukowicz evaporation model
Extended Zeldowich NO formation model
Lund flamelet model of soot formation

used in the modelling were taken from measurements on a real engine (Jamrozik 2015; Tutak, Jamrozik 2014; Tutak 2014) and on the basis of literature (Heywood 2011). These are presented in Table 4. In the case of an IC engine as a cyclic working machine, the conditions of the end of one cycle are partially also the initial conditions of the next cycle. Some of the initial parameters were difficult to measure on a real engine, they were taken from the end of a calculated cycle, e.g. initial turbulence kinetic energy and dissipation of turbulence. Boundary conditions for cylinder walls, valves and ports are taken from literature (Heywood 2011; Jamrozik 2015; Tutak, Jamrozik 2014; Tutak 2014) and are presented in Table 4. During the experimental investigation recorded pressure data as a function of the position of the crankshaft. Based on pressure data all other parameters were determined as temperature and then HRR.

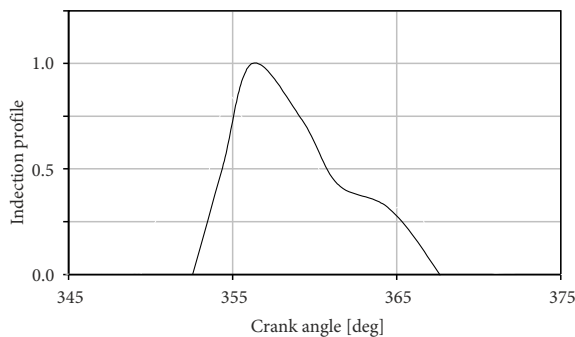


Figure 3. Injection profile

Table 4. Initial and boundary conditions

Initial pressure	0.108 MPa
Initial temperature	315 K
Piston temperature	500 K
Head temperature	390 K
Liner temperature	450 K
Start of injection	8.5 deg bTDC
End of injection	5 deg aTDC
Mass of fuel injection	$4.52 \cdot 10^{-5}$ kg
Injection type	single injection

4. Results and discussion

Simulations have been performed by employing various mesh resolutions in order to assess the mesh independence of the results. In the following analysed cases, densification of mesh is used in order to obtain independent modelling results of the mesh density (Tutak, Jamrozik 2016). Local and temporary densification of the mesh was used. The local mesh densification was used in the gap between the valve and the valve seat and in the vicinity of this area. This density was necessary at the beginning of the intake stroke where the gap was 0.3 mm and the gradients of velocity and pressure are high. When the flow field in the gap was already a relatively high the densification

could be omitted without noticeable effect on the results. Such procedure allows a significant reduces the calculation time. The used mesh is generated with a minimum cell size equal to 0.25 mm and maximal cell size of 2 mm (Figure 4). The obtained modelling results are compared to the results of the experiment.

The obtained modelling results are compared to the results of the experiment. HRR was calculated on the basis of in-cylinder pressure data and CA readings. The basis for determining the HRR was the first law of thermodynamics and the equation of state. After rearranging and simplifications, the HRR vs. CA is obtained in the well-known form as follows:

$$HRR = \frac{1}{\kappa - 1} \cdot \left(\kappa \cdot p \frac{dV}{d\phi} + V \frac{dp}{d\phi} \right),$$

where: κ – is the ratio of specific heats; V – cylinder volume; p – in-cylinder pressure; ϕ – crank angle.

Instantaneous cylinder volume V is precisely described by the engine geometry. Due to the omission as follows: heat transfer to walls, crevice volume, blow-by and the fuel injection effect, the resulted HRR is termed as the net HRR.

In Figure 5 are presented the results of model validation. To model validation used the courses of pressure from the real test engine. The diesel engine model of the AVL FIRE software, pretty accurately reflects the real processes in the CI engine. The satisfactory qualitative and quantitative compatibility occurred between the pressure courses.

In Figure 6 are presented the differences between pressure courses obtained by modelling and experiment. The maximal difference obtained in case of 50% of E85 fuel fraction an it above 12.5%. The smallest difference was for diesel fuel powering and it was 4%. It can be stated that with the increase of E85 fuel in the energetic share the difference was noticed higher. It was probably due to difficulties in the co-firing of two fuels with the use of a relatively simple mechanism. In case of the engine powered by diesel fuel the maximum difference in pressure was equal to 0.248 MPa, at 20% E85 it was 0.46 MPa and at 50% of E85 it was equal to 0.75 MPa. These biggest differences were noticed during the phase with increasing pressure during the combustion phase. The differences in pressures during the compression stroke are due to neglecting the crevice and small differences in mapping of the engine cylinder geometry. In Table 5 the comparison of peak values of pressure are presented and the HRR obtained by using modelling and experimental approach. Generally it can be stated that differences of peak pressures are rather small and the highest difference is noticed in case of 50% of E85 which was equal to 0.287 MPa which is 3% of p_{max} .

For the pressure rise and the HRR a quite good agreement is achieved as well. In case of HRR the differences are caused by the differential parts of equations based on the calculation of HRR. It can also be noted that the model does not perfectly reflect ignition delay in case of

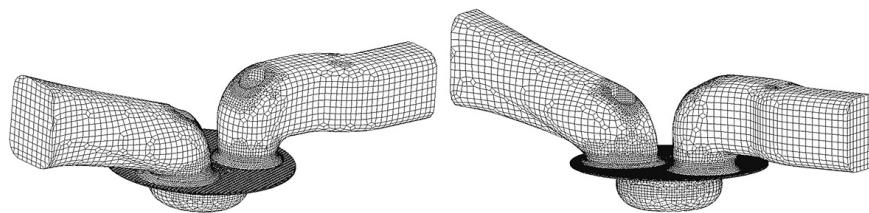


Fig. 4. View of the computational domain

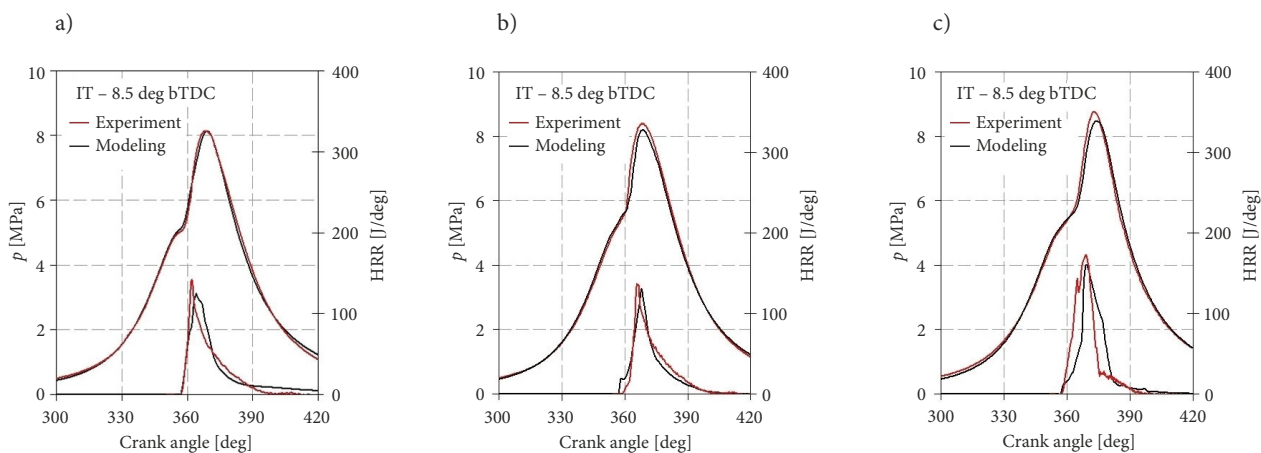


Figure 5. Comparison between experimental and computational results for in-cylinder pressure and HRR: a – pure diesel; b – 20% E85; c – 50% E85

co-combustion of both fuels. The greatest compatibility of results was achieved for the engine powered by diesel fuel. In case of an engine fed with diesel fuel, in both modelling and experimentally the HRR occurs in two visible steps: in the premixed and the diffusion phase. In case of 50% energetic share of E85 in both cases a visible reduction can be noticed in the diffusion phase of the combustion process. In this case the combustion process takes place practically only at the premixed stage as in a spark ignition engine. Piston engines are considered in terms of engine performance and in terms of toxic exhaust emissions. The main thermodynamic parameters which describe engine performance are IMEP and ITE.

4.1. Thermodynamic parameters

The thermal cycle modelling of the test engine carried out for three – consistent with the experiment – energetic shares of bioethanol fuel E85 0, 20 and 50%. The calculations started at TDC at the beginning of the intake stroke, proceeded through the total cycle of 720 degrees and finished at the end of the engine exhaust stroke.

In Figure 7 the pressure traces of diesel and DF engine are presented. It can be stated that with the increase of energetic share of bioethanol fuel E85 obtained the highest values of peak pressure. With 50% of E85 the maximum peak pressure, at 23.5 deg bTDC of diesel fuel start of injection was over 30% larger than in case of the diesel engine.

In Figure 8 the normalized heat releases of diesel and DF engine are presented. These data are used to determine

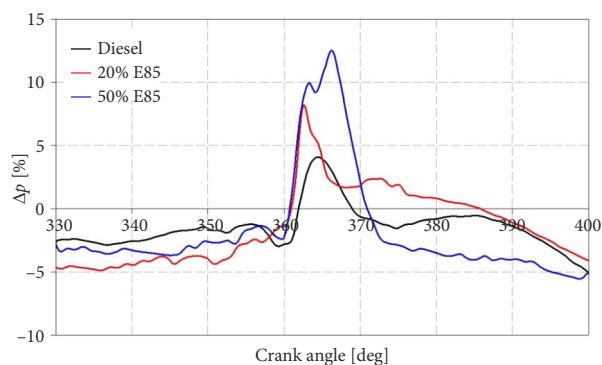


Figure 6. The combustion pressure difference obtained by modelling and by experiment

Table 5. Peak values of pressure and HRR

		p_{max} [MPa]	Angle of p_{max} [deg aTDC]	HRR _{max} [J/deg]	Angle of HRR _{max} [deg aTDC]
Diesel	Model	8.143	10	124	4
	Experimental	8.145	8	157.6	2
20% E85	Model	8.019	11	130.6	8
	Experimental	8.196	9	136.5	6
50% E85	Model	8.478	14	159.9	9
	Experimental	8.765	12	172.9	9

the phases of the combustion process. In a diesel engine as well as in a DF engine the information of ignition delay and combustion duration are essential parameters in engine control. The combustion process in the compression-ignition engine takes place in three stages. The first stage is ignition delay which is determined as the period of time in which preliminary reactions occurs of premixed charges.

The ignition delay period ends with auto-ignition. In this period the heating of the fuel droplets occurs before chemical reaction starts. To auto-ignition phenomena an appreciable amount of fuel evaporated and well mixed with air are required. In case of a dual-fuel engine, as mentioned previously, instead of air a mixture of air-fuel is delivered into the combustion chamber and the diesel fuel, which is injected into the combustion chamber evaporates in the environment of air-fuel mixture. Alcohol fuel has a high value of the heat of evaporation, which adversely affects the ignition delay time. On the other hand once ignited air-alcohol mixture tends to burn very rapidly. The second phase of combustion is known as premixed combustion phase and ends at the point of peak pressure. The third combustion phase is beginning at the point of maxi-

mum pressure but the end of this period is difficult to determine. Additionally alcohol fuel contains oxygen atoms in the particle, which has an influence on the combustion process, and it causes the reduction of the diffusion phase of the combustion.

In Figure 9 the combustion phases are presented. It can be stated that with an increase of alcohol participating in the energy dose of the fuel the ignition delay increased. On the basis of the modelling results it can be stated that during the change of the injection angle the difference was near to constant. Another dependency was noted in case of the combustion duration. For 20% energetic share of E85 fuel we observed a significant reduction in the combustion duration. In case of a conventional diesel engine operated with injection angle equal to 8.5 deg bTDC, the combustion duration reached 58 deg and in case of a DF engine with 20% of E85 this duration was equal to 26 deg. Replacement of diesel fuel by E85 in 20% resulted in the shortening of the combustion duration more than 2-times. Similar results were obtained during the experimental research of the authors (Tutak, Jamrozik 2014; Tutak et al. 2015).

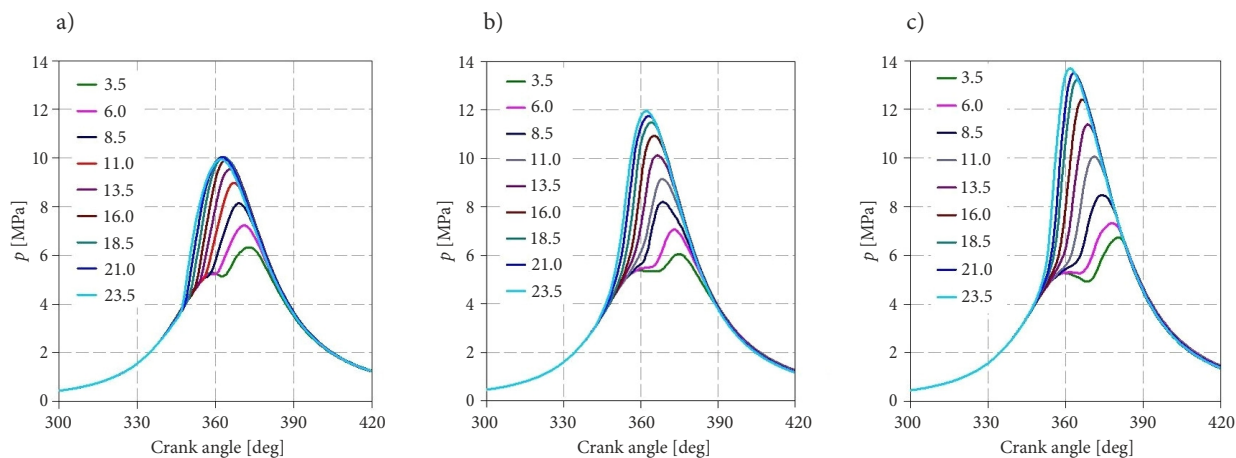


Figure 7. Pressure traces of diesel (a) and DF engine with 20% E85 (b) and 50% E85 (c), according to the angle of start of diesel fuel injection

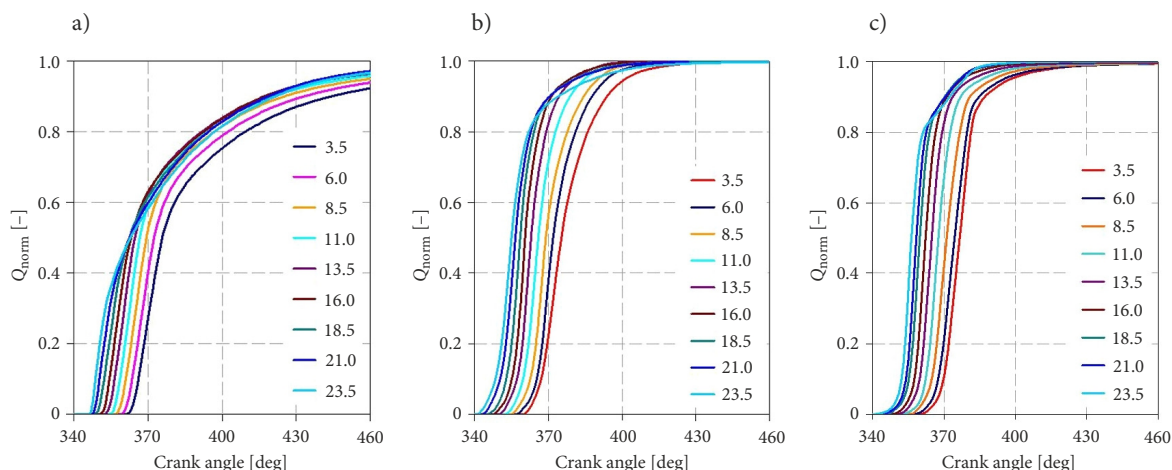


Figure 8. Normalized heat release of diesel (a) and DF engine with 20% E85 (b) and 50% E85 (c), according to the angle of start of diesel fuel injection

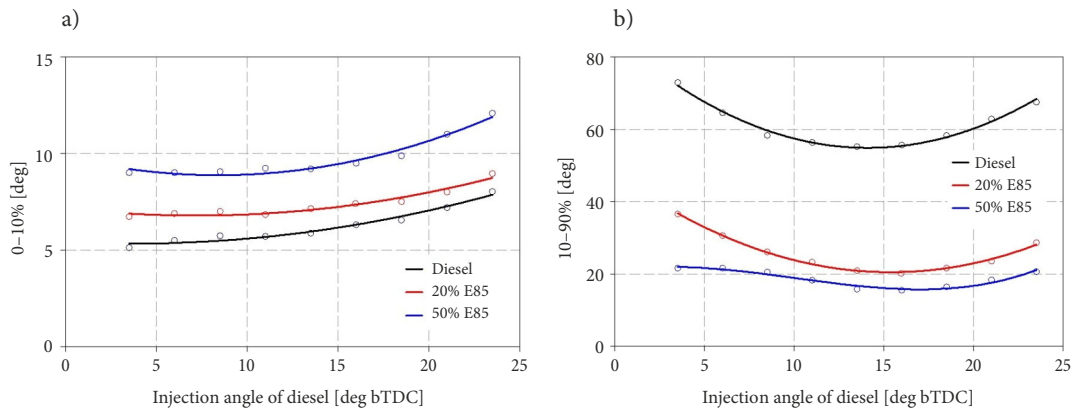


Figure 9. Combustion phases as a function of the angle of injection start of diesel fuel: a – ignition delay (0–10%); b – combustion duration (10–90%)

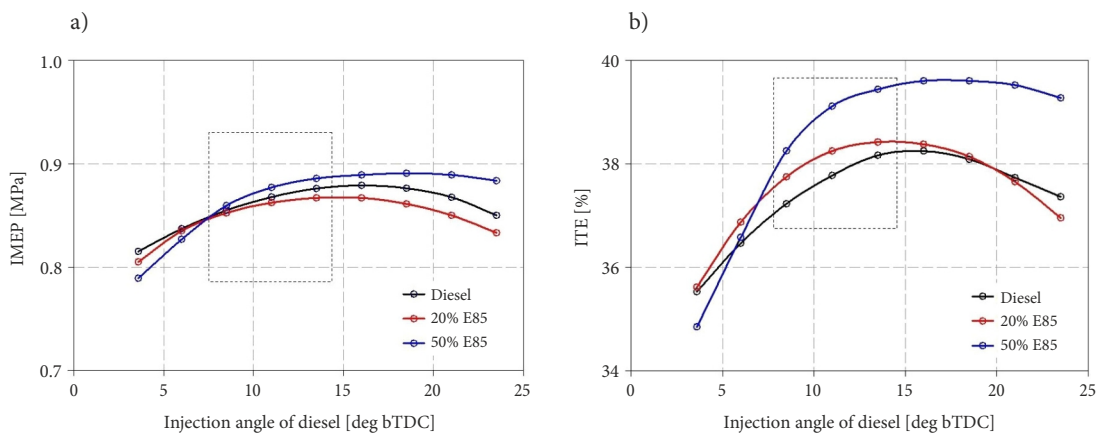


Figure 10. IMEP (a) and ITE (b) as a function of the angle of injection start of diesel fuel (the box represents the analysed cases)

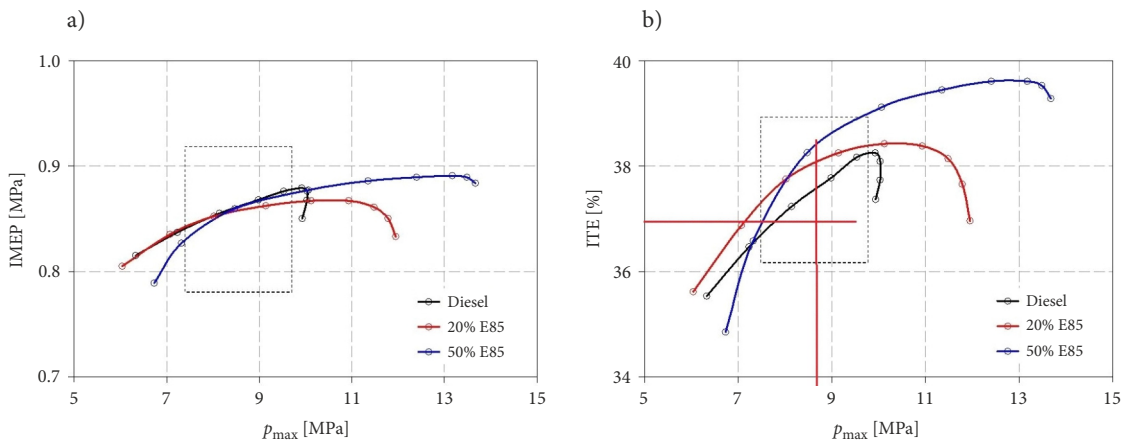


Figure 11. IMEP (a) and ITE (b) versus maximum value of pressure (the box represents the analysed cases)

In Figure 10 the IMEP and efficiency are presented. In Figure 9a the mean effective pressure versus injection angle of diesel is shown. It can be stated that the differences in IMEP are rather small, especially in so far as relevant for operational reasons of the engine. In the analysed cases for the engine powered by diesel fuel and with an energetic share of E85 fuel with the same energetic value of fuel dose, generally with larger energetic share of E85 a higher value of efficiency can be obtained. For diesel and DF engines with 20% of E85 the differences in efficiency

were rather small but in case with a 50% energetic share of E85 the increase in efficiency was definitely noticeable (Figure 10b).

In Figure 11 the IMEP and efficiency versus peak pressure are presented. It can be stated that in case of a DF engine for the same value of peak pressure p_{max} the higher value of efficiency can be obtained or otherwise in case of a DF engine the same value of efficiency can be obtained with smaller value of peak pressure (marked by red line in Figure 10b). It is beneficial for mechanical loads

of engine parts. In case of the interdependence of mean effective pressure and peak pressure in all analysed cases, in range of the relevant space for operational reasons, is almost the same. In case of a DF engine, the range of p_{\max} is larger than in case of a diesel engine. With an increase of p_{\max} the increase of IMEP was noticed, but the increase of IMEP was disproportionately small to p_{\max} growth.

4.2. Toxic components

DF combustion with alcohol fuels can reduce pollutant emissions. However, to reach the emission reduction, it may require some modifications on the engine. The IT has a significant effect on the engine performance and the emissions of CI engines (Tutak, Jamrozik 2014; Tutak et al. 2015). The performed simulations of the combustion process have provided information on the spatial and temporal distributions of the selected quantities within the combustion chamber of the test engine, especially according to toxic component formation. Before using the model to evaluate the toxicity of exhaust gases the validation process was carried out. For this purpose, the experimental data of exhaust emission is compared to those obtained by modelling. During the experimental studies information was provided on the exhaust toxicity for one angle of start of injection of diesel fuel (8.5 deg bTDC) for all modelled cases.

In Figure 12 is presented the model validation in terms of toxic components: soot and NO. As the result of experimental studies it was obtained NO_x concentration while in case of modelling obtained NO. The measurement error of NO_x was equal to 0.25 g/kWh and in case of soot emission it was near to 0.12 g/kWh for load of IMEP = 8.5 bar. Comparing the emissions of NO and NO_x obtained by modelling and experiment in case of an engine supplied with diesel emissions were higher near to 15%. A similar difference is obtained for the engine co-firing diesel and E85 fuel. In case of soot emission the highest difference was noticed for engine powered by diesel fuel and it was equal to 30%. The differences in soot emissions of DF engine were lower and these did not exceed 15%. However, NO_x consists primarily of NO, it seems that this comparison is justified. Both the experiment and the modelling resulted in very similar trend of

changes in emissions of NO and NO_x in the test engine. The same with soot, with a higher energetic share of E85 model results were closer to those obtained experimentally. For example, at 20% of energetic share of E85 by modelling an emission of NO of 10% lower value was obtained than during experiment. At the same point, soot emission was lower by 13%. Considering the complexity of the processes, occurring in the ICE and the fact, that it was a DF engine, these results seem to be satisfactory.

The NO_x formation rate has a strong relationship with temperature. The high NO_x formation rate in the combustion chamber of an ICE is due to high temperature in the combustion chamber during premixed combustion phase (Barik, Murugan 2014). This combustion phase can be decreased by injection strategy which can cause a decrease in peak temperature and thus in NO_x emissions. Lower temperature in the combustion chamber causes lower thermal efficiency of the engine and in addition this can result in increased soot emissions. The soot emission is related to the diffusion phase. The formation of NO occurs most intensively in burn gases, which represents the main source of emission (Appel et al. 2000; Ma et al. 2014; Reşitoğlu et al. 2015). This thermal mechanism of NO formation is described by highly temperature-dependent chemical reactions known as the extended Zeldovich mechanism. By the temperature over 2200 K the production rate of NO_x is doubled for every 90 K. In DF engines, the value of peak temperature can be reduced by using fuels with high value of heat of evaporation. This property of the fuel causes a decrease of the temperature of in-cylinder charge before the start of the combustion and as a consequence decreases maximum temperature during the burning process. In the combustion chamber of the diesel engine are zones with very poor and very rich mixtures. The rich fuel zones cause a strong tendency to soot formation. The mechanism of soot formation is very complex and the effect on soot particles formed the influence of both chemical and physical processes. A temperature of 1600 K is a certain limit in the formation of soot, below this temperature the soot formation process is intensive but above this temperature oxidation processes start to dominate (Bockhorn 1994). During the computation the Lund flamelet model was used to calculate soot emission. This model calculates the soot volume fraction source terms, integrated over the probability density function of the mixture fraction, as a function of the scalar dissipation rate, pressure and temperature on the oxidizer side (AVL LIST GmbH 2013). During the calculation surface growth, oxidation, particle inception and fragmentation are considered.

In Figure 13 is presented the effect of DF combustion on emission characteristics. In case of soot emission it can be stated that with the increase of the injection angle the soot emission is decreased but after reaching the CA of diesel injection 20 deg bTDC the emission of soot started to grow. Additionally, it can be stated that with the increase of the energetic participation of E85 the soot emission is decreased at all ranges of the analysed operations of the engine. The opposite relationship was obtained in case of NO emission. With the increase of E85 in the fuel

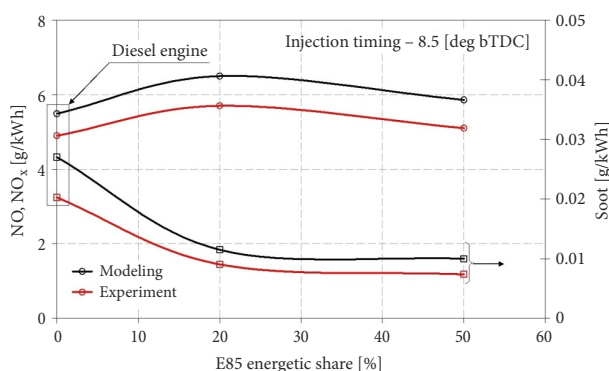


Figure 12. Model validation in terms of exhaust emissions

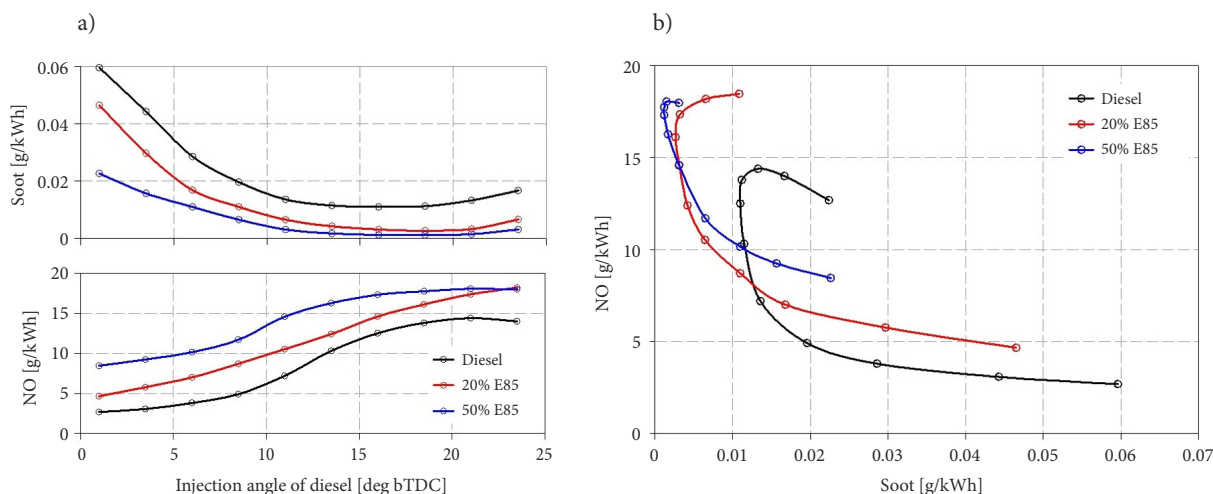


Figure 13. Soot and NO emission (a) and interdependence of soot and NO emission (b) as a function of the angle of injection start of diesel fuel

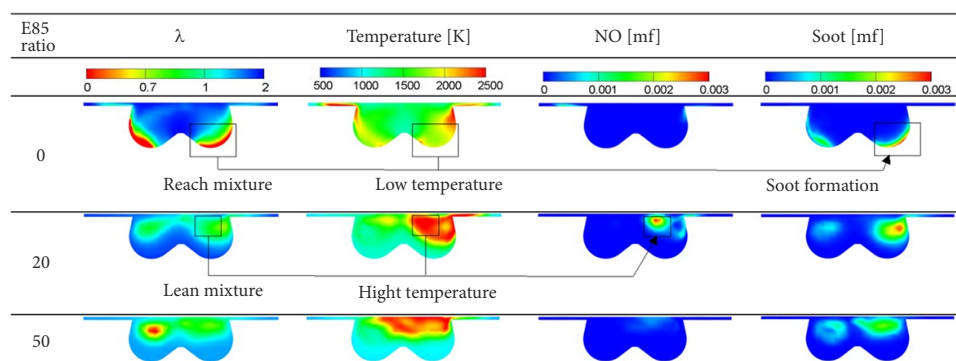


Figure 14. The cross sections of the combustion chamber at 5 deg aTDC of piston position, presented: excess air ratio (λ), temperature, NO and soot emission at the engine

the emission of NO increased. The values of emissions are comparable with values obtained during the experimental researches, with injection angle equal to 8.5 deg bTDC (Tutak, Jamrozik 2014; Tutak *et al.* 2015). In Figure 13b the interdependence of soot and NO emission is presented. On the basis of this chart it can be stated that the emission of soot and NO are opposed to each other.

In all analysed cases achieved conditions in which soot emission starts to grow back with lower NO emission. It is associated with the achievement of the optimum thermodynamic parameters of the thermal cycle. In the real engine it was not possible to operate at that point because of knock combustion.

In Figure 14 are marked the areas in which NO and soot formation process take place. From the drawings it can be seen that the NO is formed where the temperature and excess air occur simultaneously. In the case of soot emissions, to the formation of soot the presence of fuel is required at a relatively low temperature which is visible in Figure 14. From the Fig 14 can be seen that the NO_x is formed where the high temperature and excess air occur simultaneously. In the case of soot emissions, to the creation of excess fuel is required at a relatively low temperature.

Conclusions

The paper presents the results of a DF diesel engine modelling with the use of CFD software. To create an appropriate mesh required many simulations, in order to become independent of calculation results on the mesh density. The performed simulations of the combustion process provided information on the spatial and temporal distribution of the selected quantities within the combustion chamber of the test engine, especially with respect to toxic component formation. This information would be extremely difficult to obtain by experimental methods. Observations regarding the thermodynamic and operating parameters of DF engines:

- with the increase of energetic share of bioethanol fuel E85 the highest values of peak pressure were noticed;
- with the increase of alcohol participating in the energy dose of fuel the ignition delay increased. Another dependency was noted in case of the combustion duration. Replacement of diesel fuel by E85 in 20% resulted in the shortening of the combustion duration more than 2-times;

- with equal energetic value of fuel dose, generally with larger energetic share of E85 a higher value of efficiency was obtained. For diesel and DF engines with 20% of E85 the differences in efficiency were rather small but in case with 50% energetic share of E85 the increase in efficiency was definitely noticeable;
- in case of DF engines for the same value of peak pressure p_{\max} a higher value of efficiency can be obtained, or otherwise in case of DF engine the same value of efficiency can be obtained with a smaller value of peak pressure;
- in case of DF engines the range of p_{\max} is larger than in case of conventional diesel engines. With an increase of p_{\max} the increase of IMEP was noticed, but the increase of IMEP was disproportionately small to p_{\max} growth.

Observations regarding toxic exhaust emissions:

- with the increase of the injection angle the soot emission is decreased but after reaching the CA of diesel injection 20 deg bTDC emission of soot started to grow;
- with the increase of energetic participation of E85 the soot emission is decreased at all ranges of the analysed operations of the engine. The opposite relationship was observed in case of NO emission;
- with the increase of E85 in the fuel the emission of NO increased. The values of emissions are comparable with the values obtained during the experimental researches, with an injection angle equal to 8.5 deg bTDC;
- emission of soot and NO are opposed to each other. In all analysed cases achieved conditions in which soot emission starts to grow back with lower NO emission. It is associated with the achievement of the optimum thermodynamic parameters of the thermal cycle.

It turned out that the engine model with an acceptable accuracy was suitable for the modelling of emissions. This model also confirmed that the dynamics of soot formation is opposed to NO_x formation. In summary, CFD modelling has fulfilled its role as a powerful tool to optimize the IC, both in terms of thermodynamic parameters and emissions.

Acknowledgements

The authors would like to express their gratitude to AVL LIST GmbH for providing an AVL FIRE software under the University Partnership Program.

Disclosure Statement

Authors have not any competing financial, professional, or personal interests from other parties.

References

- Abu-Qudais, M.; Haddad, O.; Qudaisat, M. 2000. The effect of alcohol fumigation on diesel engine performance and emissions, *Energy Conversion and Management* 41(4): 389–399. [https://doi.org/10.1016/S0196-8904\(99\)00099-0](https://doi.org/10.1016/S0196-8904(99)00099-0)
- Appel, J.; Bockhorn, H.; Frenklach, M. 2000. Kinetic modeling of soot formation with detailed chemistry and physics: laminar premixed flames of C_2 hydrocarbons, *Combustion and Flame* 121(1–2): 122–136. [https://doi.org/10.1016/S0010-2180\(99\)00135-2](https://doi.org/10.1016/S0010-2180(99)00135-2)
- AVL LIST GmbH. 2013. *AVL FIRE: User Manual*. V 2013.1. Graz, Austria.
- Barik, D.; Murugan, S. 2014. Simultaneous reduction of NO_x and smoke in a dual fuel DI diesel engine, *Energy Conversion and Management* 84: 217–226. <https://doi.org/10.1016/j.enconman.2014.04.042>
- Bockhorn, H. 1994. *Soot Formation in Combustion: Mechanisms and Models*. Springer. 597 p. <https://doi.org/10.1007/978-3-642-85167-4>
- Can, Ö.; Çelikten, İ.; Usta, N. 2004. Effects of ethanol addition on performance and emissions of a turbocharged indirect injection Diesel engine running at different injection pressures, *Energy Conversion and Management* 45(15–16): 2429–2440. <https://doi.org/10.1016/j.enconman.2003.11.024>
- Colin, O.; Benkenida, A. 2004. The 3-zones extended coherent flame model (ecfm3z) for computing premixed/diffusion combustion, *Oil & Gas Science and Technology – Revue d'IFP Energies nouvelles* 59(6): 593–609. <https://doi.org/10.2516/ogst:2004043>
- EC. 2009. *Directive 2009/28/EC of the European Parliament and of the Council of 23 April 2009 on the Promotion of the Use of Energy from Renewable Sources and Amending and Subsequently Repealing Directives 2001/77/EC and 2003/30/EC*. 47 p. Available from Internet: <http://eur-lex.europa.eu/legal-content/EN/TXT/PDF/?uri=CELEX:32009L0028&from=EN>
- Heywood, J. 2011. *Internal Combustion Engine Fundamentals*. Tata McGraw Hill Education. 960 p.
- Irimescu, A.; Marchitto, L.; Merola, S. S.; Tornatore, C.; Valentino, G. 2015. Combustion process investigations in an optically accessible DISI engine fuelled with *n*-butanol during part load operation, *Renewable Energy* 77: 363–376. <https://doi.org/10.1016/j.renene.2014.12.029>
- Jamrozik, A. 2015. Lean combustion by a pre-chamber charge stratification in a stationary spark ignited engine, *Journal of Mechanical Science and Technology* 29(5): 2269–2278. <https://doi.org/10.1007/s12206-015-0145-7>
- Jamrozik, A. 2009. Modelling of two-stage combustion process in SI engine with prechamber, in *MEMSTECH 2009: 2009 5th International Conference on Perspective Technologies and Methods in MEMS Design – 2009*, 22–24 April 2009, Zakarpattya, Ukraine, 13–16.
- Jamrozik, A.; Tutak, W. 2014. Theoretical analysis of air-fuel mixture formation in the combustion chambers of the gas engine with two-stage combustion system, *Bulletin of the Polish Academy of Sciences Technical Sciences: the Journal of Polish Academy of Sciences* 62(4): 779–790. <https://doi.org/10.2478/bpasts-2014-0085>
- Jamrozik, A.; Tutak, W. 2011. A study of performance and emissions of SI engine with a two-stage combustion system, *Chemical and Process Engineering: the Journal of Committee of Chemical and Process of Polish Academy of Sciences* 32(4): 453–471. <https://doi.org/10.2478/v10176-011-0036-0>

- Jamrozik, A.; Tutak, W. 2010. Modelling of combustion process in the gas test engine, in *2010 Proceedings of V1th International Conference on Perspective Technologies and Methods in MEMS Design (MEMSTECH)*, 20–23 April 2010, Lviv, Ukraine, 14–17.
- Jamrozik, A.; Tutak, W.; Kociszewski, A.; Sosnowski, M. 2013. Numerical simulation of two-stage combustion in SI engine with prechamber, *Applied Mathematical Modelling* 37(5): 2961–2982. <https://doi.org/10.1016/j.apm.2012.07.040>
- Jamrozik, A.; Tutak, W.; Pyrc, M.; Sobiepański, M. 2017. Effect of diesel-biodiesel-ethanol blend on combustion, performance, and emissions characteristics on a direct injection diesel engine, *Thermal Science* 21(1): 591–604. <https://doi.org/10.2298/TSCI160913275J>
- Kim, B.; Yoon, W.; Ryu, S.; Ha, J. 2005. Effect of the injector nozzle hole diameter and number on the spray characteristics and the combustion performance in medium-speed diesel marine engines, *SAE Technical Paper* 2005-01-3853. <https://doi.org/10.4271/2005-01-3853>
- Labeckas, G.; Slavinskas, S.; Mažeika, M. 2014. The effect of ethanol–diesel–biodiesel blends on combustion, performance and emissions of a direct injection diesel engine, *Energy Conversion and Management* 79: 698–720. <https://doi.org/10.1016/j.enconman.2013.12.064>
- Lebedevas, S.; Lebedeva, G.; Žaglinskis, J.; Rapalis, P.; Gudaitytė, I. 2013. Research of characteristics of working cycle of high-speed diesel engine operating on biofuels RME–E and D–RME–E. Part 2. Indicators and characteristics of heat release in diesel cylinder, *Transport* 28(3): 217–223. <https://doi.org/10.3846/16484142.2013.828652>
- López, J. J.; Novella, R.; García, A.; Winklinger, J. F. 2013. Investigation of the ignition and combustion processes of a dual-fuel spray under diesel-like conditions using computational fluid dynamics (CFD) modeling, *Mathematical and Computer Modelling* 57(7–8): 1897–1906. <https://doi.org/10.1016/j.mcm.2011.12.030>
- Luft, S. 2010. A dual-fuel compression ignition engine – distinctive features, *Combustion Engines* (2): 33–39.
- Ma, S.; Zheng, Z.; Liu, H.; Zhang, Q.; Yao, M. 2013. Experimental investigation of the effects of diesel injection strategy on gasoline/diesel dual-fuel combustion, *Applied Energy* 109: 202–212. <https://doi.org/10.1016/j.apenergy.2013.04.012>
- Ma, Y.; Zhu, M.; Zhang, D. 2014. Effect of a homogeneous combustion catalyst on the characteristics of diesel soot emitted from a compression ignition engine, *Applied Energy* 113: 751–757. <https://doi.org/10.1016/j.apenergy.2013.08.028>
- Merola, S. S.; Tornatore, C.; Iannuzzi, S. E.; Marchitto, L.; Valentino, G. 2014. Combustion process investigation in a high speed diesel engine fuelled with *n*-butanol diesel blend by conventional methods and optical diagnostics, *Renewable Energy* 64: 225–237. <https://doi.org/10.1016/j.renene.2013.11.017>
- Morsy, M. H. 2015. Assessment of a direct injection diesel engine fumigated with ethanol/water mixtures, *Energy Conversion and Management* 94: 406–414. <https://doi.org/10.1016/j.enconman.2015.01.086>
- Padala, S.; Woo, C.; Kook, S.; Hawkes, E. R. 2013. Ethanol utilisation in a diesel engine using dual-fuelling technology, *Fuel* 109: 597–607. <https://doi.org/10.1016/j.fuel.2013.03.049>
- Rakopoulos, C. D.; Antonopoulos, K. A.; Rakopoulos, D. C.; Hountalas, D. T. 2008a. Multi-zone modeling of combustion and emissions formation in DI diesel engine operating on ethanol–diesel fuel blends, *Energy Conversion and Management* 49(4): 625–643. <https://doi.org/10.1016/j.enconman.2007.07.035>
- Rakopoulos, D. C.; Rakopoulos, C. D.; Kakaras, E. C.; Giakoumis, E. G. 2008b. Effects of ethanol–diesel fuel blends on the performance and exhaust emissions of heavy duty DI diesel engine, *Energy Conversion and Management* 49(11): 3155–3162. <https://doi.org/10.1016/j.enconman.2008.05.023>
- Raslavičius, L.; Bazaras, Ž. 2010. The possibility of increasing the quantity of oxygenates in fuel blends with no diesel engine modifications, *Transport* 25(1): 81–88. <https://doi.org/10.3846/transport.2010.11>
- Raslavičius, L.; Bazaras, Ž. 2009. The analysis of the motor characteristics of D–RME–E fuel blend during on-field tests, *Transport* 24(3): 187–191. <https://doi.org/10.3846/1648-4142.2009.24.187-191>
- Reşitoğlu, İ. A.; Altinişik, K.; Keskin, A. 2015. The pollutant emissions from diesel-engine vehicles and exhaust aftertreatment systems, *Clean Technologies and Environmental Policy* 17(1): 15–27. <https://doi.org/10.1007/s10098-014-0793-9>
- Şahin, Z.; Durgun, O. 2013. Improving of diesel combustion-pollution-fuel economy and performance by gasoline fumigation, *Energy Conversion and Management* 76: 620–633. <https://doi.org/10.1016/j.enconman.2013.07.068>
- Şahin, Z.; Durgun, O.; Kurt, M. 2015. Experimental investigation of improving diesel combustion and engine performance by ethanol fumigation-heat release and flammability analysis, *Energy Conversion and Management* 89: 175–187. <https://doi.org/10.1016/j.enconman.2014.09.053>
- Sarathy, S. M.; Oßwald, P.; Hansen, N.; Kohse-Höinghaus, K. 2014. Alcohol combustion chemistry, *Progress in Energy and Combustion Science* 44: 40–102. <https://doi.org/10.1016/j.pecc.2014.04.003>
- Sarjoavaara, T.; Larmi, M. 2015. Dual fuel diesel combustion with an E85 ethanol/gasoline blend, *Fuel* 139: 704–714. <https://doi.org/10.1016/j.fuel.2014.09.049>
- Sarjoavaara, T.; Alantie, J.; Larmi, M. 2013. Ethanol dual-fuel combustion concept on heavy duty engine, *Energy* 63: 76–85.
- Sarjoavaara, T.; Larmi, M.; Vuorinen, V. 2015. Effect of charge air temperature on E85 dual-fuel diesel combustion, *Fuel* 153: 6–12. <https://doi.org/10.1016/j.fuel.2015.02.096>
- Sayin, C.; Canakci, M. 2009. Effects of injection timing on the engine performance and exhaust emissions of a dual-fuel diesel engine, *Energy Conversion and Management* 50(1): 203–213. <https://doi.org/10.1016/j.enconman.2008.06.007>
- Siwale, L.; Lukács, K.; Torok, A.; Bereczky, A.; Mbarawa, M.; Penninger, A.; Kolesnikov, A. 2013. Combustion and emission characteristics of *n*-butanol/diesel fuel blend in a turbo-charged compression ignition engine, *Fuel* 107: 409–418. <https://doi.org/10.1016/j.fuel.2012.11.083>
- Splitter, D. A.; Reitz, R. D. 2014. Fuel reactivity effects on the efficiency and operational window of dual-fuel compression ignition engines, *Fuel* 118: 163–175. <https://doi.org/10.1016/j.fuel.2013.10.045>
- Tutak, W. 2014. Bioethanol E85 as a fuel for dual fuel diesel engine, *Energy Conversion and Management* 86: 39–48. <https://doi.org/10.1016/j.enconman.2014.05.016>
- Tutak, W.; Jamrozik, A. 2016. Validation and optimization of the thermal cycle for a diesel engine by computational fluid dynamics modeling, *Applied Mathematical Modelling* 40(13–14): 6293–6309. <https://doi.org/10.1016/j.apm.2016.02.021>
- Tutak, W.; Jamrozik, A. 2014. Generator gas as a fuel to power a diesel engine, *Thermal Science* 18(1): 205–216. <https://doi.org/10.2298/TSCI130228063T>

- Tutak, W.; Jamrozik, A. 2011. Characteristics of the flow field in the combustion chamber of the internal combustion test engine, *Chemical and Process Engineering* 32(3): 203–214.
<https://doi.org/10.2478/v10176-011-0016-4>
- Tutak, W.; Jamrozik, A.; Kociszewski, A. 2011. Improved emission characteristics of SI test engine by EGR, in *2011 Proceedings of VIIIth International Conference on Perspective Technologies and Methods in MEMS Design (MEMSTECH)*, 11–14 May 2011, Polyana, Ukraine, 101–103.
- Tutak, W.; Lukács, K.; Szwaja, S.; Bereczky, Á. 2015. Alcohol-diesel fuel combustion in the compression ignition engine, *Fuel* 154: 196–206.
<https://doi.org/10.1016/j.fuel.2015.03.071>
- Valentino, G.; Iannuzzi, S.; Marchitto, L.; Merola, S.; Tornatore, C. 2014. Optical investigation of postinjection strategy effect at the exhaust line of a light-duty diesel engine supplied with diesel/butanol and biodiesel blends, *Journal of Energy Engineering* 140(3).
[https://doi.org/10.1061/\(ASCE\)EY.1943-7897.0000155](https://doi.org/10.1061/(ASCE)EY.1943-7897.0000155)
- Vallinayagam, R.; Vedharaj, S.; Yang, W. M.; Saravanan, C. G.; Lee, P. S.; Chua, K. J. E.; Chou, S. K. 2014. Impact of pine oil biofuel fumigation on gaseous emissions from a diesel engine, *Fuel Processing Technology* 124: 44–53.
<https://doi.org/10.1016/j.fuproc.2014.02.012>
- Wei, L.; Geng, P. 2016. A review on natural gas/diesel dual fuel combustion, emissions and performance, *Fuel Processing Technology* 142: 264–278.
<https://doi.org/10.1016/j.fuproc.2015.09.018>
- Zhang, Z. H.; Cheung, C. S.; Chan, T. L.; Yao, C. D. 2009. Emission reduction from diesel engine using fumigation methanol and diesel oxidation catalyst, *Science of the Total Environment* 407(15): 4497–4505.
<https://doi.org/10.1016/j.scitotenv.2009.04.036>
- Zhang, Z. H.; Cheung, C. S.; Chan, T. L.; Yao, C. D. 2010. Experimental investigation of regulated and unregulated emissions from a diesel engine fueled with Euro V diesel fuel and fumigation methanol, *Atmospheric Environment* 44(8): 1054–1061.
<https://doi.org/10.1016/j.atmosenv.2009.12.017>
- Zöldy, M. 2011. Ethanol–biodiesel–diesel blends as a diesel extender option on compression ignition engines, *Transport* 26(3): 303–309.
<https://doi.org/10.3846/16484142.2011.623824>
- Zöldy, M.; Török, Á. 2015. Road transport liquid fuel today and tomorrow: literature overview, *Periodica Polytechnica Transportation Engineering* 43(4): 172–176.
<https://doi.org/10.3311/PPtr.8095>